Astronomy & Astrophysics

LETTER TO THE EDITOR

The reddening law of type Ia supernovae: separating intrinsic variability from dust using equivalent widths[⋆]

The Nearby Supernova Factory:

N. Chotard[1], E. Gangler[1], G. Aldering[2], P. Antilogus[3], C. Aragon[2], S. Bailey[2], C. Baltay[4], S. Bongard[3], C. Buton[5], A. Canto[3], M. Childress[2,6], Y. Copin[1], H. K. Fakhouri[2,6], E. Y. Hsiao[2], M. Kerschhaggl[5], M. Kowalski[5], S. Loken[2], P. Nugent[7,8], K. Paech[5], R. Pain[3], E. Pecontal[9], R. Pereira[1], S. Perlmutter[2,6], D. Rabinowitz[4], K. Runge[2], R. Scalzo[4,10], G. Smadja[1], C. Tao[11,12], R. C. Thomas[7], B. A. Weaver[13], and C. Wu[3,14]

[1] Université de Lyon, Université Lyon 1, CNRS/IN2P3, Institut de Physique Nucléaire de Lyon, 69622 Villeurbanne, France
 e-mail: nchotard@ipnl.in2p3.fr
[2] Physics Division, Lawrence Berkeley National Laboratory, 1 Cyclotron Road, Berkeley, CA 94720, USA
[3] LPNHE, Université Pierre et Marie Curie Paris 6, Université Paris Diderot Paris 7, CNRS-IN2P3, 75252 Paris Cedex 05, France
[4] Department of Physics, Yale University, New Haven, CT 06250-8121, USA
[5] Physikalisches Institut Universitat Bonn, Nussallee 12 53115 Bonn, Germany
[6] Department of Physics, University of California Berkeley, 366 LeConte Hall MC 7300, Berkeley, CA, 94720-7300, USA
[7] Computational Cosmology Center, Lawrence Berkeley National Laboratory, 1 Cyclotron Road, Berkeley, CA 94720, USA
[8] Department of Astronomy, University of California, Berkeley, CA 94720-3411, USA
[9] Observatoire de Lyon, 69230 Saint-Genis Laval, Université de Lyon, Université Lyon 1, 69003 Lyon, France
[10] Australian National University, Mt. Stromlo Observatory, The RSAA, Weston Creek, ACT 2611, Australia
[11] Centre de Physique des Particules de Marseille, 163 avenue de Luminy, Case 902, 13288 Marseille Cedex 09, France
[12] Tsinghua Center for Astrophysics, Tsinghua University, Beijing 100084, PR China
[13] New York University, Center for Cosmology and Particle Physics, 4 Washington Place, New York, NY 10003, USA
[14] National Astronomical Observatories, Chinese Academy of Sciences, Beijing 100012, PR China

ABSTRACT

We employ 76 type Ia supernovae (SNe Ia) with optical spectrophotometry within 2.5 days of B-band maximum light obtained by the Nearby Supernova Factory to derive the impact of Si and Ca features on the supernovae intrinsic luminosity and determine a dust reddening law. We use the equivalent width of Si II λ4131 in place of the light curve stretch to account for first-order intrinsic luminosity variability. The resulting empirical spectral reddening law exhibits strong features that are associated with Ca II and Si II λ6355. After applying a correction based on the Ca II H&K equivalent width we find a reddening law consistent with a Cardelli extinction law. Using the same input data, we compare this result to synthetic rest-frame $UBVRI$-like photometry to mimic literature observations. After corrections for signatures correlated with Si II λ4131 and Ca II H&K equivalent widths and introducing an empirical correlation between colors, we determine the dust component in each band. We find a value of the total-to-selective extinction ratio, $R_V = 2.8 \pm 0.3$. This agrees with the Milky Way value, in contrast to the low R_V values found in most previous analyses. This result suggests that the long-standing controversy in interpreting SN Ia colors and their compatibility with a classical extinction law, which is critical to their use as cosmological probes, can be explained by the treatment of the dispersion in colors, and by the variability of features apparent in SN Ia spectra.

Key words. supernovae: general – dust, extinction – cosmology: observations

1. Introduction

Type Ia supernovae (SNe Ia) luminosity distances are measured via the standardization of their light curves using brightness-width (stretch, x_1, Δm_{15}) and color corrections (Phillips 1993; Tripp 1998; Guy et al. 2007; Jha et al. 2007). While the determination of the intrinsic dispersion related to the light curve shape is subject to small differences between fitters, the manner in which color is linked to dust is still controversial, because it may be affected by additional yet unidentified intrinsic dispersion. Whereas earlier work used the total-to-selective extinction ratio of the Milky Way, $R_V = 3.1$, direct estimates from

the supernovae (SNe) Hubble diagram fits lead to lower values, from $R_V = 1.7$ to $R_V = 2.5$ (Hicken et al. 2009; Tripp 1998; Wang et al. 2009). While the derivation of this value is subject to assumptions about the natural color dispersion of SNe (Freedman et al. 2009; Guy et al. 2010), the reason for a difference between SNe data and the Milky Way average result have remained unknown.

Equivalent widths are good spectral indicators for addressing this question because they probe the intrinsic variability of SNe Ia and by construction little depend on extinction owing to their narrow wavelength baseline. Arsenijevic et al. (2008) showed a strong correlation between the equivalent width of the Si II λ4131 feature and the SALT2 x_1 width parameter (Guy et al. 2007), and Bronder et al. (2008) showed its correlation with M_B.
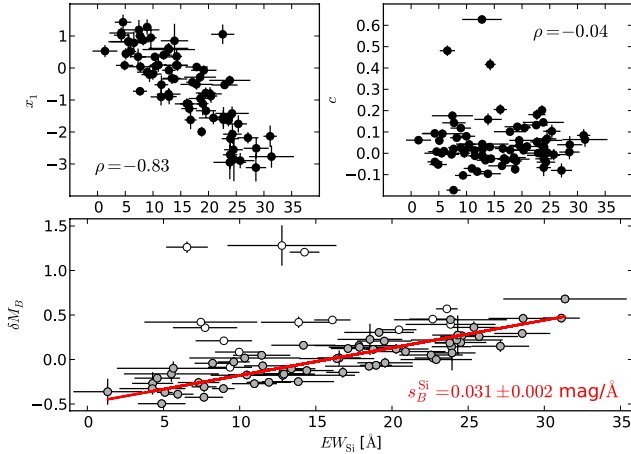
Fig. 1. Correlations of EW^{Si}, SALT2 x_1 (*top left*) and c (*top right*) parameters and measured peak absolute magnitude up to a constant term, δM_B (*bottom*). The open circles in the *bottom panel* are the data points excluded from the fit, which is displayed as a solid line. s_B^{Si} is equivalent for the B-band to the red curve shown in Fig. 3a.

Walker et al. (2011) used it to standardize the Hubble diagram, but were hindered from drawing firm conclusions by the quality of the low redshift data.

In this work, we take advantage of the Nearby Supernova Factory (SNfactory) spectrophotometric sample to revisit these conclusions, using both spectral data and derived $UBVRI$-like synthetic photometry. We present in Sect. 2 the SNe Ia sample and the definition of the Si II λ4131 and Ca II H&K equivalent widths, which will be used in Sect. 3.1 to correct the Hubble residuals. These corrected magnitudes are used to derive the relative absorption in each wavelength band, δA_λ. The correlations between the δA_λ from SN to SN across different bands provide the reddening law, as described in Sect. 3.2, as well as the dispersion matrix between bands. In Sect. 4 we show that the resulting reddening law agrees with a Cardelli extinction law (CCM, Cardelli et al. 1989; O'Donnell 1994). Our reddening law has a value of R_V which agrees with the Milky-Way value of 3.1, when the proper dispersion matrix is used. We then discuss these results in Sect. 5 and conclude in Sect. 6.

2. Data set and derived quantities

This analysis uses flux calibrated spectra of 76 SNe Ia obtained by the SNfactory collaboration with its SNIFS instrument (Aldering et al. 2002) on the University of Hawaii 2.2-m telescope on Mauna Kea. This subset is selected in the same way as in Bailey et al. (2009), using only SNe with a measured spectrum within 2.5 days of B-band maximum, but with an enlarged data set with a redshift range of $0.007 < z < 0.09$. The SALT2 x_1 and c parameters (Fig. 1) and the spectra phases with respect to the B-band maximum light are derived using fits of the full light curves in three observer-frame top hat bandpasses corresponding approximately to BVR.

After flux calibration, host galaxy subtraction, and correction for Milky Way extinction, the 76 spectra are transformed into rest frame. For the spectral analysis, they are rebinned with a resolution of 1500 km s^{-1}. In addition, synthetic magnitudes are derived from the spectra after photon integration in a set of five $UBVRI$-like top-hat bandpasses with a constant resolution over the whole spectral range ($3276-8635$ Å, see Fig. 3 and caption). The uncorrected Hubble residuals $\delta M(\lambda) = M(\lambda) - \langle M(\lambda) \rangle$ are independently computed for each band of mean wavelength λ, relative to a flat ΛCDM universe with $\Omega_M = 0.28$ and

$H_0 = 70$ km s^{-1} Mpc^{-1}. For the spectral analysis, the Hubble residuals are corrected for phase dependence using linear interpolation. For broad bands, we instead interpolate the magnitudes to the date of the B-maximum, using the light curve shape of each SN Ia as defined by the SALT2 x_1 parameter, but with each band's peak magnitude fitted separately. The data are presented in Table 1. The errors on Hubble residuals include statistical, calibration ($\sim$2% for peak luminosity), and redshift uncertainties. They are correlated between bands with a correlation coefficient varying from 0.64 to 0.98.

The equivalent widths EW^{Si} and EW^{Ca} corresponding to the Si II λ4131 and the Ca II H&K features are computed in the same way as in Bronder et al. (2008), Eq. (1)). The errors are derived using a Monte Carlo procedure that takes into account photon noise and the impact of the method used to select the feature boundaries. EW^{Si} and EW^{Ca} are insensitive to extinction by dust, changing by less than 1% when adding an artificial reddening with a CCM law with $R_V = 3.1$ and $E(B-V) = 0.5$.

3. Method

3.1. Intrinsic corrections and absorption measurements

The Hubble residuals exhibit a dependency on observables such as EW^{Si} and EW^{Ca}, which are uncorrelated with dust extinction. As shown in Fig. 1 as an example, the δM_B dependence on EW^{Si} exhibits a linear behavior, with an asymmetrical magnitude dispersion attributed to extinction and remaining intrinsic variability. A similar dependence with equivalent widths is found for other bands. We may thus model the Hubble residuals for a given SN, i, as a sum of intrinsic and dust components, making various assumptions about the number of spectral energy distribution (SED) correction vectors, s_λ, from none (Eq. (1a)) to two (Eq. (1c)):

$$\delta M_{\lambda,i} = \begin{cases} \delta A_{\lambda,i}^0 & \text{(1a)} \\ EW_i^{Si} s_\lambda^{Si} + \delta A_{\lambda,i}^{Si} & \text{(1b)} \\ EW_i^{Si} s_\lambda^{Si} + EW_i^{Ca} s_\lambda^{Ca} + \delta A_{\lambda,i}^{Si+Ca}. & \text{(1c)} \end{cases}$$

After finding s_λ^{Si} and the $\delta A_{\lambda,i}^{Si}$ by a least-squares minimization over all SNe from Eq. (1b), with an asymmetrical 2σ clipping, s_λ^{Si} is kept constant and s_λ^{Ca} and the $\delta A_{\lambda,i}^{Si+Ca}$ are then computed in the same manner. An example of the fit using EW^{Si} for the B-band is given is Fig. 1 (solid line), s_B^{Si} being the correction applied to find the $\delta A_{B,i}^{Si}$.

3.2. The empirical reddening law

Because we expect the relation between the δA_λ to be linear for dust extinction, as shown in Fig. 2 for the U- and V-bands, we model the empirical reddening law as

$$\delta A_{\lambda,i} = \gamma_\lambda \, \delta A_{V,i}^* + \eta_\lambda, \tag{2}$$

where $\delta A_{\lambda,i}$ are the measured values, the slopes γ_λ ($=\partial A_\lambda / \partial A_V^*$) the reddening law coefficients, $\delta A_{V,i}^*$ the fitted relative extinction for the SN i, and η_λ a free zero point. $\delta A_{V,i}^*$, γ_λ and η_λ are obtained by a χ^2 fit using the full wavelength covariance matrix C_i of the $\delta A_{\lambda,i}$ measurements. However, the data are more dispersed than their measurement error (Fig. 2), and another source of dispersion must be introduced. We adopt an iterative approach by using the fit residuals, $r_{\lambda,i} = \delta A_{\lambda,i} - (\gamma_\lambda \, \delta A_{V,i}^* + \eta_\lambda)$, to determine the covariance remaining after accounting for the measurement
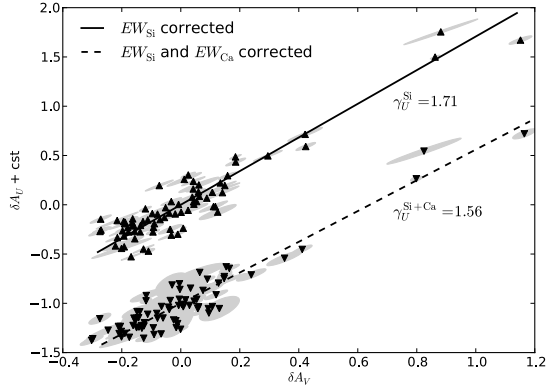
Fig. 2. Relation between δA_U and δA_V after $\mathrm{EW}^{\mathrm{Si}}$ correction (triangles up) and after $\mathrm{EW}^{\mathrm{Si}}$ and $\mathrm{EW}^{\mathrm{Ca}}$ corrections (triangles down). The δA_U are displayed with an added arbitrary constant. The ellipses represent the full measured covariance matrix between the two bands. They are enlarged by the additional subtraction error after $\mathrm{EW}^{\mathrm{Ca}}$ correction. The result of the fits are also displayed. The γ_U^{Si} and $\gamma_U^{\mathrm{Si}+\mathrm{Ca}}$ respectively correspond to the ones in Figs. 3b and c for the U-band.
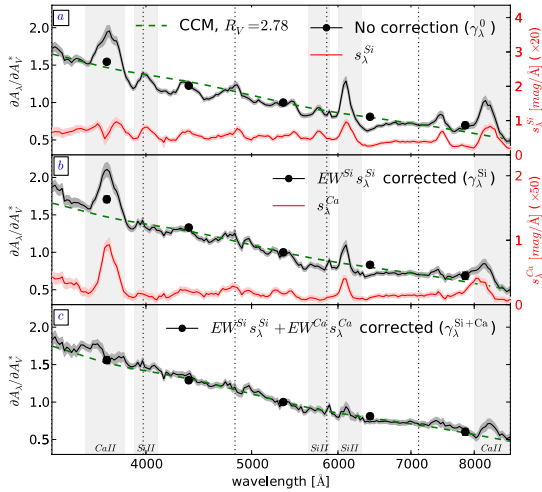

Fig. 3. Black: reddening law presented as $\gamma_\lambda \equiv \partial A_\lambda / \partial A_V^*$ as a function of wavelength. Filled circles correspond to the results obtained using the $UBVRI$-like bands, curves are for the spectral analysis. Red: linear slope s_λ (mag/Å) of equivalent widths versus δM_λ. Dotted lines: CCM law fit corresponding to the broad bands analysis. *Panel* **a):** δM_λ corrected only for the phase dependence (Eq. (1a)). *Panel* **b):** δM_λ corrected for phase and $\mathrm{EW}^{\mathrm{Si}}$ (Eq. (1b)). *Panel* **c):** δM_λ corrected for phase, $\mathrm{EW}^{\mathrm{Si}}$ and $\mathrm{EW}^{\mathrm{Ca}}$ (Eq. (1c)). The vertical dotted lines represent the $UBVRI$-like bands boundaries. The shaded vertical bands represent the Si and Ca domain. The shaded band around the curves are the statistical errors.

error covariance, $C_{\lambda_1 \lambda_2, i}$. This empirical covariance matrix, D, is given by

$$D_{\lambda_1 \lambda_2} = \frac{1}{N} \sum_{i=1}^{N} \left(r_{\lambda_1, i}\, r_{\lambda_2, i} - C_{\lambda_1 \lambda_2, i} \right) \qquad (3)$$

where N is the number of SNe. In the next iteration, the total covariance matrix is given by $C_i + D$. We have checked that the converged matrix does not depend on initial conditions.

4. Results

4.1. EW$^{\mathrm{Si}}$ and EW$^{\mathrm{Ca}}$ impacts on the derived extinction law

Results for the SED correction vector, s_λ, and the reddening law, γ_λ, are presented in Fig. 3 for different assumptions about the number of intrinsic components. If SNe were perfect standard candles affected only by dust as assumed by Eq. (1a) and Fig. 3a, the empirical reddening law γ_λ^0 would be a CCM-like law with an average R_V for our galaxy sample. However, γ_λ^0 clearly exhibits small-scale SN-like features. These features correlate strongly with some of the features in the $\mathrm{EW}^{\mathrm{Si}}$ correction spectrum, s_λ^{Si}, derived via Eq. (1b) and illustrated in red in Fig. 3a.

The reddening law obtained after $\mathrm{EW}^{\mathrm{Si}}$ correction (Fig. 3b) is closer to a CCM law, except in the Ca $\textsc{ii}$ H&K and IR triplet, and the Si $\textsc{ii}$ $\lambda 6355$ region. This indicates the presence of a second source of intrinsic variability. We select $\mathrm{EW}^{\mathrm{Ca}}$ to trace a second spectral correction vector, $s_\lambda^{\mathbf{Ca}}$ (Eq. (1c)), since Ca is clearly a major contributor to the observed variability and $\mathrm{EW}^{\mathrm{Ca}}$ and $\mathrm{EW}^{\mathrm{Si}}$ also happen to be uncorrelated ($\rho = 0.06 \pm 0.12$). As shown in Fig. 3b, $s_\lambda^{\mathbf{Ca}}$ does a good job of reproducing the shape of the deviation of γ_λ^{Si} relative to the CCM law.

The mean reddening law, γ_λ^{Si+Ca}, obtained after the additional correction by $\mathrm{EW}^{\mathrm{Ca}}$ (Fig. 3c) is a much smoother curve with small residual features and agrees well with a CCM extinction law. Thus it appears that these two components can account for SN Ia spectral variations at optical wavelengths. Any intrinsic component that might remain would have to be largely uncorrelated with SN spectral features fixed in wavelength, as well as being coincidentally compatible with a CCM law.

4.2. R_V determination

We apply the same treatment as above to our $UBVRI$-like synthetic photometric bands, and find agreement with the spectral analysis, as shown by the black points in the three panels in Fig. 3. After the $\mathrm{EW}^{\mathrm{Si}}$ correction (Eq. (1b), Fig. 3b), the U- and I-band values deviate significantly from a CCM law, which is recovered after the full $\mathrm{EW}^{\mathrm{Si}}$ and $\mathrm{EW}^{\mathrm{Ca}}$ correction (Eq. (1c), Fig. 3c). The empirical fit presented in Sect. 3.2 can be forced to follow a CCM extinction law by substituting $\delta A_{\lambda, i} = (a_\lambda + b_\lambda / R_V)\, \delta A_{V, i}^* + \eta_\lambda$, where a_λ and b_λ are the wavelength-dependent parameters given in Cardelli et al. (1989) and O'Donnell (1994), and a single R_V is fit over all bands. This fit applied to δA_λ^{Si+Ca} leads to an average $R_V = 2.78 \pm 0.34$ for the SN host galaxies in our sample. This value is compatible with the Milky Way average of $R_V = 3.1$ The quoted uncertainty is statistical and derived with a jackknife procedure, removing one supernova at a time.

We tested the robustness of our R_V determination in several ways. Since the s_λ are measured in sequence, each one using the corrected magnitudes from the previous step, we swap the order in which the correction is applied, and find $R_V = 2.70$. Using the whole sample to compute the s_λ instead of applying a 2σ clipping cut leads to $R_V = 2.79$, which shows the small influence of clipping at this stage. Host galaxy subtraction is performed using the full spatio-spectral information from the host obtained after the SN Ia has faded, and we do not see evidence for residual host galaxy features in our spectra. The measurement covariance matrix C_i depends on the assumed calibration accuracy: for the present result, this is estimated from repeated measurements of standard stars. Another estimate can be obtained from the residuals to a SALT2 light-curve fit. Using this in C_i values leads to $R_V = 2.76$. The stability of the result with respect to our choice of bandpasses is checked by removing one band at a time, and we obtain a rms of ± 0.23 around the mean result. Finally, a Monte Carlo simulation was performed using the converged γ_λ, $\delta A_{V,i}^*$, η_λ and dispersion matrix D as an input, and setting $R_V = 2.78$. The $\delta A_{\lambda, i}$ are then randomly generated adding Gaussian noise with covariance $C_i + D$. Over 100 generations, the D matrix is

recovered with a maximal bias of 5% on the diagonal elements and the mean fitted value is $R_V = 2.68 \pm 0.03$, indicating that, if anything, our method slightly underestimates R_V.

5. Discussion

In this work, we selected EW^{Si} as a first variable for correction because it provides a good proxy for x_1, and it because is a model-independent variable. In our data-set the Pearson correlation coefficient of EW^{Si} with x_1 is -0.83 ± 0.04 (Fig. 1), which confirms the result found in Arsenijevic et al. (2008). Computing the Hubble residuals in the B-band using (x_1, c) or $(\text{EW}^{\text{Si}}, c)$ to standardize SNe both lead to a dispersion of residuals of 0.16 mag, also confirming this result. We find that EW^{Si} is uncorrelated with c ($\rho = -0.04 \pm 0.12$, Fig. 1), contrary to the recent claim by Nordin et al. (2010). Because EW^{Si} and x_1 are highly correlated, it is possible to redo the analysis with x_1 in place of EW^{Si}. The resulting SED correction vector $s_\lambda^{x_1}$ is similar to s_λ^{Si}, and the conclusions identical, yielding $R_V = 2.69$.

Computing the Hubble residuals with $(\text{EW}^{\text{Si}}, \text{EW}^{\text{Ca}}, c)$ to standardize supernovae leads to a dispersion of 0.15 mag, which is a small improvement. Indeed, we do observe a correlation of EW^{Ca} and c, with $\rho = 0.34 \pm 0.10$. This correlation is even increased to $\rho = 0.50$ when c is computed with a U-band in addition to BVR in the light-curve fit. This shows that c contains an intrinsic component, and that the SALT2 analysis is already accounting for some of this Ca effect. This is illustrated in Fig. 3b: the SALT2 color model is derived taking into account a variability measured by one intrinsic parameter only, and thus can be compared to $\gamma_\lambda^{\text{Si}}$. The observed U-band contribution in broad filters explains the UV rise in the empirical color models. The presence of a second intrinsic parameter induces an increased variability in the UV, as was already noticed by Ellis et al. (2008), but without a clear attribution to the Ca II H&K line.

Much lower effective R_V values have been found previously: $R_V = 1.1$ in Tripp (1998), $R_V = 2.2$ in Kessler et al. (2009); Guy et al. (2010) and $R_V \approx 1-2$ in Folatelli et al. (2010). These values were derived accounting only for one intrinsic parameter beyond color. If we derive an effective value after the sole EW^{Si} correction to mimic these analyses, we obtain $R_V = 3.1$, so the explanation for the difference has little to do with the number of intrinsic parameters entering the correction. This difference is explained by the assumption on the dispersion matrix. Indeed, if we instead use the one of Guy et al. (2010), corresponding to an rms between 0.09 and 0.11 mag on the diagonal, and all off-diagonal terms with an identical rms of 0.09 mag, we obtain $R_V = 1.86$. This value is representative of previous analyses, but the matrix used is incompatible with our best-fit matrix. D has diagonal values of 0.07, 0.04, 0.05, 0.05 and 0.10 for $UBVRI$ respectively, lower than the values quoted by Guy et al. (2010). However, while adjacent bands are correlated in our matrix, an anti-correlation growing to -1 when the wavelength difference increases is observed for other bands, which implies a large color dispersion. As shown by Freedman et al. (2009) and Kessler et al. (2009), increasing the color dispersion leads to a higher R_V value. This long-range anti-correlation implies that uncorrected variability in the SN spectra and/or the reddening law remains.

6. Conclusions

Equivalent widths are essentially independent of host reddening and provide a handle on the intrinsic properties of the SNe Ia.

In particular, EW^{Si} measured at maximum light is confirmed to be as powerful as stretch. After correction for this intrinsic contribution to the magnitude, we derived a reddening law and proposed a natural method to assess the dispersion caused by additional fluctuations. We found that this empirical reddening law is affected by features linked to the SN physics, and showed that the Ca II H&K line provides a second intrinsic variable that is uncorrelated with EW^{Si} or x_1. Correcting Hubble residuals with EW^{Si} and EW^{Ca} leads to a reddening law consistent with a canonical CCM extinction law, while adding a dispersion in colors during the fit leads to a value of R_V close to the Milky Way value of 3.1. Owing to the coupling of R_V with the residual dispersion matrix, the derived value of R_V may be affected as the remaining variability becomes better understood and corrected. Our plan to study the same SNe Ia over a range of phases should help address this issue. The evolution of SNe Ia will be one of the main limitations to their use in precision cosmology surveys at high redshift. Our findings show that the accurate measurements of the Ca II H&K line provides an additional tool to improve the separation of dust and intrinsic variability. The presence of remaining scatter offers the possibility of improvements in the future.

References

Aldering, G., Adam, G., Antilogus, P., et al. 2002, SPIE Conf., 4836, 61
Arsenijevic, V., Fabbro, S., Mourão, A. M., et al. 2008, A&A, 492, 535
Bailey, S., Aldering, G., Antilogus, P., et al. 2009, A&A, 500, L17
Bronder, T. J., Hook, I. M., Astier, P., et al. 2008, A&A, 477, 717
Cardelli, J. A., Clayton, G. C., & Mathis, J. S. 1989, ApJ, 345, 245
Cooke, J., Ellis, R. S., Sullivan, M., et al. 2011, ApJ, 727, L35
Ellis, R. S., Sullivan, M., Nugent, P. E., et al. 2008, ApJ, 674, 51
Folatelli, G., Phillips, M. M., Burns, C. R., et al. 2010, AJ, 139, 120
Freedman, W. L., Burns, C. R., Phillips, M. M., et al. 2009, ApJ, 704, 1036
Guy, J., Astier, P., Baumont, S., et al. 2007, A&A, 466, 11
Guy, J., Sullivan, M., Conley, A., et al. 2010, A&A, 523, A7
Hicken, M., Challis, P., Jha, S., et al. 2009, ApJ, 700, 331
Jha, S., Riess, A. G., & Kirshner, R. P. 2007, ApJ, 659, 122SNe Ia.
SNe Ia. Kessler, R., Becker, A. C., Cinabro, D., et al. 2009, ApJS, 185, 32
Nordin, J., Ostman, L., Goobar, A., et al. 2010 [arXiv:1012.4430]
O'Donnell, J. E. 1994, ApJ, 422, 158
Phillips, M. M. 1993, ApJ, 413, L105
Tripp, R. 1998, A&A, 331, 815
Walker, E. S., Hook, I. M., Sullivan, M., et al. 2011, MNRAS, 410, 1262
Wang, X., Filippenko, A. V., Ganeshalingam, M., et al. 2009, ApJ, 699, L139

Table 1. Supernovae used in this work, including synthetic magnitudes after phase correction δM_λ, SALT2 fit parameters x_1 and c, equivalent widths EW^{Si} and EW^{Ca} in Å and phases in days.

Name	z_{cmb}^1	δM_U	δM_B	δM_V	δM_R	δM_I	x_1	c	EW^{Si}	EW^{Ca}	Phase
SN2004ef[a]	0.0298	0.408 ± 0.012	0.357 ± 0.010	0.249 ± 0.010	0.208 ± 0.009	0.148 ± 0.010	−1.62 ± 0.29	0.181 ± 0.024	22.7 ± 1.5	140.4 ± 2.5	0.5 ± 0.2
SNF20050728-006	0.0582	0.428 ± 0.065	0.322 ± 0.064	0.239 ± 0.064	0.202 ± 0.063	0.161 ± 0.064	0.85 ± 0.53	0.159 ± 0.027	13.9 ± 2.5	144.6 ± 6.2	−0.9 ± 0.4
SNF20051022-006	0.0449	−0.153 ± 0.051	−0.124 ± 0.050	−0.096 ± 0.051	−0.013 ± 0.050	0.030 ± 0.051	0.95 ± 0.35	0.000 ± 0.021	9.6 ± 1.1	127.5 ± 2.4	0.7 ± 0.4
SNF20060511-014	0.0466	−0.002 ± 0.085	−0.079 ± 0.085	−0.029 ± 0.085	−0.102 ± 0.084	−0.022 ± 0.086	−1.27 ± 0.15	0.022 ± 0.022	16.5 ± 1.4	101.3 ± 11.2	0.6 ± 0.1
SNF20060526-003	0.0787	−0.068 ± 0.025	−0.049 ± 0.023	−0.066 ± 0.023	−0.009 ± 0.022	−0.004 ± 0.023	−0.90 ± 0.27	0.013 ± 0.017	11.4 ± 1.9	121.3 ± 6.1	−0.8 ± 0.3
SNF20060621-015	0.0541	−0.443 ± 0.027	−0.368 ± 0.026	−0.300 ± 0.026	−0.218 ± 0.026	−0.189 ± 0.026	0.09 ± 0.21	−0.071 ± 0.015	11.0 ± 1.5	106.9 ± 7.7	1.1 ± 0.3
SN2006dm[b]	0.0208	0.381 ± 0.017	0.368 ± 0.015	0.331 ± 0.015	0.295 ± 0.014	0.275 ± 0.015	−2.13 ± 0.34	0.084 ± 0.030	31.1 ± 1.2	101.1 ± 2.7	−1.3 ± 0.2
SN2006do[b]	0.0274	0.163 ± 0.014	0.170 ± 0.012	0.152 ± 0.012	0.149 ± 0.012	0.253 ± 0.034	−2.86 ± 0.68	0.003 ± 0.036	24.6 ± 1.0	117.7 ± 2.5	−0.6 ± 0.4
SNF20060911-014	0.0887	−0.468 ± 0.126	−0.365 ± 0.126	−0.318 ± 0.126	−0.228 ± 0.126	−0.187 ± 0.126	1.02 ± 0.21	−0.040 ± 0.015	4.3 ± 1.4	80.3 ± 9.4	−0.8 ± 0.4
SNF20060919-007	0.0694	−0.229 ± 0.039	−0.168 ± 0.037	−0.126 ± 0.038	−0.098 ± 0.037	−0.069 ± 0.038	−0.52 ± 0.29	−0.012 ± 0.018	11.5 ± 1.2	125.9 ± 2.4	−0.4 ± 0.7
SNF20061020-000	0.0372	0.252 ± 0.069	0.264 ± 0.068	0.269 ± 0.068	0.146 ± 0.068	0.044 ± 0.068	−1.75 ± 0.27	0.103 ± 0.031	25.4 ± 1.6	97.3 ± 8.4	0.9 ± 0.5
SNF20061021-003	0.0615	0.190 ± 0.038	0.114 ± 0.037	−0.017 ± 0.037	−0.016 ± 0.037	−0.078 ± 0.038	−0.13 ± 0.14	0.118 ± 0.013	9.0 ± 1.9	123.7 ± 2.7	−0.7 ± 0.0
SNF20061024-000	0.0557	0.464 ± 0.054	0.365 ± 0.051	0.376 ± 0.051	0.298 ± 0.051	0.290 ± 0.052	−2.51 ± 0.31	0.040 ± 0.041	28.6 ± 2.3	86.3 ± 27.4	0.3 ± 0.6
SNF20061108-004	0.0879	−0.265 ± 0.020	−0.274 ± 0.017	−0.303 ± 0.017	−0.240 ± 0.017	−0.072 ± 0.039	0.58 ± 0.20	0.043 ± 0.014	12.8 ± 4.7	129.1 ± 6.7	−0.2 ± 0.0
SNF20061111-002	0.0682	0.099 ± 0.035	−0.046 ± 0.034	−0.068 ± 0.034	−0.120 ± 0.034	−0.102 ± 0.047	1.05 ± 0.31	0.132 ± 0.018	22.6 ± 2.1	112.5 ± 8.4	−0.9 ± 0.3
SN2006ob[c]	0.0582	0.114 ± 0.017	0.196 ± 0.014	0.226 ± 0.015	0.174 ± 0.014	0.127 ± 0.015	−3.11 ± 0.44	0.006 ± 0.034	28.5 ± 1.8	92.0 ± 14.0	0.0 ± 0.4
SNF20070403-001	0.0815	−0.046 ± 0.015	−0.008 ± 0.012	−0.027 ± 0.013	−0.019 ± 0.012	0.079 ± 0.036	−1.56 ± 0.20	0.032 ± 0.014	20.9 ± 2.6	97.9 ± 16.4	−0.0 ± 0.3
SN2007bd[d]	0.0320	−0.202 ± 0.021	−0.162 ± 0.019	−0.097 ± 0.019	−0.093 ± 0.019	−0.108 ± 0.037	−1.12 ± 0.37	−0.036 ± 0.024	19.0 ± 1.0	108.8 ± 8.8	−0.4 ± 0.4
SNF20070424-003	0.0680	0.138 ± 0.045	0.063 ± 0.044	0.102 ± 0.044	0.088 ± 0.044	0.024 ± 0.055	0.09 ± 0.11	0.029 ± 0.013	14.2 ± 2.1	128.5 ± 4.9	0.5 ± 0.1
SNF20070427-001	0.0778	−0.761 ± 0.016	−0.521 ± 0.013	−0.352 ± 0.013	−0.235 ± 0.013	−0.228 ± 0.015	−0.73 ± 0.13	−0.173 ± 0.012	7.7 ± 1.3	84.8 ± 3.1	−0.5 ± 0.3
SNF20070506-006	0.0355	−0.471 ± 0.063	−0.404 ± 0.063	−0.407 ± 0.063	−0.329 ± 0.063	−0.308 ± 0.063	1.00 ± 0.14	0.021 ± 0.017	7.7 ± 0.8	95.3 ± 1.9	−0.1 ± 0.1
SNF20070531-011	0.0358	0.078 ± 0.060	0.047 ± 0.059	0.085 ± 0.059	0.072 ± 0.059	0.137 ± 0.063	−2.71 ± 0.43	−0.067 ± 0.040	23.9 ± 1.3	112.4 ± 13.8	0.3 ± 0.6
SN2007cq[e]	0.0246	−0.299 ± 0.082	−0.260 ± 0.082	−0.279 ± 0.082	−0.198 ± 0.082	−0.228 ± 0.082	−0.82 ± 0.18	−0.013 ± 0.019	12.8 ± 2.1	66.7 ± 6.4	−2.3 ± 0.2
SNF20070630-006	0.0706	−0.072 ± 0.029	−0.080 ± 0.028	−0.021 ± 0.028	−0.035 ± 0.028	−0.029 ± 0.028	0.35 ± 0.13	0.027 ± 0.013	10.3 ± 3.6	139.4 ± 5.1	1.1 ± 0.2
SNF20070701-005	0.0683	−0.311 ± 0.045	−0.261 ± 0.044	−0.250 ± 0.044	−0.263 ± 0.044	−0.178 ± 0.044	−0.89 ± 0.24	0.021 ± 0.019	12.9 ± 1.4	105.0 ± 2.8	0.0 ± 0.0
SNF20070712-000	0.0296	0.166 ± 0.047	0.111 ± 0.046	0.079 ± 0.046	0.080 ± 0.045	0.140 ± 0.046	−0.78 ± 0.17	0.060 ± 0.022	19.5 ± 1.8	93.1 ± 8.2	2.2 ± 0.0
SNF20070712-003	0.0738	−0.240 ± 0.042	−0.221 ± 0.041	−0.130 ± 0.041	−0.104 ± 0.041	−0.148 ± 0.041	0.08 ± 0.17	−0.025 ± 0.013	14.4 ± 1.8	104.2 ± 12.3	−1.8 ± 0.2
SNF20070717-003	0.0859	0.210 ± 0.022	0.122 ± 0.020	0.175 ± 0.020	0.105 ± 0.019	0.107 ± 0.021	−1.42 ± 0.22	0.060 ± 0.016	24.3 ± 3.0	112.1 ± 41.9	1.9 ± 0.2
SNF20070725-001	0.0668	−0.413 ± 0.043	−0.353 ± 0.042	−0.253 ± 0.042	−0.152 ± 0.042	−0.056 ± 0.043	0.40 ± 0.15	−0.086 ± 0.015	11.9 ± 1.5	107.2 ± 2.6	0.6 ± 0.4
SNF20070727-016	0.0665	−0.817 ± 0.029	−0.593 ± 0.027	−0.517 ± 0.027	−0.437 ± 0.027	−0.390 ± 0.028	0.08 ± 0.15	−0.053 ± 0.015	4.9 ± 1.6	80.6 ± 3.3	1.0 ± 0.5
SNF20070802-000	0.0643	0.360 ± 0.041	0.208 ± 0.041	0.144 ± 0.041	0.128 ± 0.040	0.150 ± 0.041	−0.07 ± 0.16	0.124 ± 0.012	19.2 ± 2.3	159.7 ± 4.9	0.7 ± 0.2
SNF20070803-005	0.0303	−0.647 ± 0.146	−0.459 ± 0.146	−0.487 ± 0.146	−0.422 ± 0.146	−0.455 ± 0.146	0.53 ± 0.19	0.062 ± 0.019	1.3 ± 2.3	38.8 ± 4.1	−2.0 ± 0.1
SNF20070806-026	0.0440	−0.010 ± 0.064	0.052 ± 0.063	0.118 ± 0.063	0.069 ± 0.063	0.076 ± 0.063	−2.18 ± 0.18	−0.080 ± 0.033	27.1 ± 1.9	98.4 ± 11.1	1.8 ± 0.2
SNF20070810-004	0.0827	−0.015 ± 0.030	−0.097 ± 0.029	−0.060 ± 0.029	−0.026 ± 0.029	0.031 ± 0.044	−0.53 ± 0.11	0.001 ± 0.011	22.9 ± 2.3	127.8 ± 4.8	2.2 ± 0.0
SNF20070818-001	0.0728	0.269 ± 0.041	0.059 ± 0.039	−0.011 ± 0.039	−0.017 ± 0.038	0.046 ± 0.039	−0.51 ± 0.16	0.101 ± 0.013	17.8 ± 2.9	156.0 ± 9.1	−1.2 ± 0.2
SNF20070817-003	0.0630	0.227 ± 0.176	0.129 ± 0.176	0.190 ± 0.176	0.184 ± 0.176	0.273 ± 0.179	−0.95 ± 0.15	−0.020 ± 0.014	18.6 ± 2.1	98.0 ± 4.3	1.7 ± 0.2
SN2007kk[f]	0.0406	−0.231 ± 0.017	−0.271 ± 0.015	−0.278 ± 0.015	−0.208 ± 0.014	−0.128 ± 0.015	0.06 ± 0.19	0.042 ± 0.015	10.5 ± 1.2	128.6 ± 2.1	−0.4 ± 0.3
SNF20071015-000	0.0373	1.340 ± 0.065	1.166 ± 0.064	0.876 ± 0.064	0.672 ± 0.064	0.410 ± 0.064	0.79 ± 0.35	0.481 ± 0.025	6.5 ± 1.4	102.8 ± 6.5	−1.0 ± 0.4
SN2007le[g]	0.0055	1.445 ± 0.016	1.109 ± 0.014	0.817 ± 0.014	0.723 ± 0.013	0.675 ± 0.014	0.36 ± 0.26	0.417 ± 0.027	14.3 ± 1.0	149.0 ± 2.8	−1.2 ± 0.2
SNF20071021-000	0.0262	0.471 ± 0.034	0.238 ± 0.034	0.166 ± 0.034	0.161 ± 0.034	0.220 ± 0.034	−0.88 ± 0.21	0.120 ± 0.020	20.5 ± 1.1	165.2 ± 8.0	−0.6 ± 0.1
SN2007nq[h]	0.0439	0.038 ± 0.022	0.094 ± 0.019	0.084 ± 0.019	0.038 ± 0.018	0.015 ± 0.020	−2.56 ± 0.43	0.068 ± 0.043	24.5 ± 1.7	89.7 ± 8.5	1.5 ± 0.7
SNF20080323-009	0.0834	−0.383 ± 0.017	−0.201 ± 0.015	−0.081 ± 0.015	−0.082 ± 0.014	−0.118 ± 0.017	−0.32 ± 0.18	−0.033 ± 0.016	13.4 ± 1.6	105.0 ± 4.0	0.6 ± 0.4
SNF20080510-001	0.0723	−0.166 ± 0.028	−0.172 ± 0.027	−0.116 ± 0.028	−0.075 ± 0.027	−0.039 ± 0.028	−0.29 ± 0.15	−0.028 ± 0.012	18.5 ± 2.9	117.7 ± 2.8	−0.7 ± 0.1
SNF20080512-010	0.0639	−0.149 ± 0.196	−0.023 ± 0.196	0.044 ± 0.196	0.027 ± 0.196	0.021 ± 0.196	−2.21 ± 0.28	−0.026 ± 0.026	23.9 ± 1.5	94.8 ± 4.7	0.3 ± 0.1
SNF20080514-002	0.0230	−0.130 ± 0.012	0.018 ± 0.011	0.098 ± 0.011	0.117 ± 0.011	0.078 ± 0.026	−1.99 ± 0.15	−0.075 ± 0.020	18.8 ± 0.5	81.0 ± 1.7	−0.1 ± 0.1
SNF20080516-000	0.0736	−0.395 ± 0.038	−0.306 ± 0.038	−0.290 ± 0.038	−0.204 ± 0.037	−0.214 ± 0.038	1.43 ± 0.24	0.008 ± 0.018	4.6 ± 1.5	104.9 ± 3.5	−1.2 ± 0.4
SNF20080516-022	0.0747	−0.518 ± 0.016	−0.345 ± 0.014	−0.184 ± 0.014	−0.161 ± 0.013	−0.246 ± 0.016	−0.34 ± 0.11	−0.096 ± 0.012	13.8 ± 2.4	89.2 ± 15.4	0.2 ± 0.1
SNF20080522-000	0.0463	−0.622 ± 0.060	−0.423 ± 0.059	−0.480 ± 0.059	−0.411 ± 0.059	−0.467 ± 0.059	1.09 ± 0.17	0.093 ± 0.017	4.3 ± 2.2	46.5 ± 25.0	0.7 ± 0.2

Table 1. continued.

Name	z^1_{cmb}	δM_U	δM_B	δM_V	δM_R	δM_I	x_1	c	EW^{Si}	EW^{Ca}	Phase
SNF20080522-011	0.0385	−0.421 ± 0.038	−0.424 ± 0.037	−0.393 ± 0.037	−0.345 ± 0.037	−0.361 ± 0.037	1.28 ± 0.24	0.026 ± 0.019	8.9 ± 0.7	120.3 ± 2.3	0.6 ± 0.3
SNF20080531-000	0.0368	0.072 ± 0.055	0.021 ± 0.055	0.038 ± 0.055	0.041 ± 0.055	0.079 ± 0.055	−0.81 ± 0.21	0.014 ± 0.017	20.3 ± 2.1	132.8 ± 2.6	0.5 ± 0.2
SNF20080610-000	0.0789	0.106 ± 0.017	0.041 ± 0.015	0.106 ± 0.015	0.104 ± 0.014	0.125 ± 0.016	0.03 ± 0.13	0.015 ± 0.013	17.9 ± 2.0	119.0 ± 4.9	1.0 ± 0.0
SNF20080612-003	0.0330	−0.522 ± 0.046	−0.487 ± 0.045	−0.487 ± 0.045	−0.442 ± 0.045	−0.442 ± 0.054	0.52 ± 0.20	0.010 ± 0.018	5.9 ± 1.0	121.4 ± 2.3	−0.9 ± 0.4
SNF20080614-010	0.0752	0.109 ± 0.018	0.162 ± 0.016	0.262 ± 0.016	0.167 ± 0.015	0.133 ± 0.016	−2.90 ± 0.24	−0.006 ± 0.026	25.7 ± 2.6	99.1 ± 36.8	1.3 ± 0.3
SNF20080623-001	0.0448	0.081 ± 0.026	0.027 ± 0.025	0.094 ± 0.025	0.111 ± 0.024	0.173 ± 0.025	−0.44 ± 0.13	−0.031 ± 0.013	17.1 ± 1.1	149.5 ± 1.8	0.4 ± 0.1
SNF20080626-002	0.0232	−0.290 ± 0.090	−0.258 ± 0.090	−0.267 ± 0.090	−0.168 ± 0.090	−0.112 ± 0.090	0.83 ± 0.24	0.000 ± 0.020	5.5 ± 3.1	129.1 ± 1.0	−0.1 ± 0.3
SNF20080714-008	0.0846	0.547 ± 0.038	0.350 ± 0.036	0.253 ± 0.036	0.217 ± 0.036	0.212 ± 0.044	−0.39 ± 0.15	0.145 ± 0.012	23.8 ± 3.7	120.4 ± 17.4	0.2 ± 0.2
SN2008ec[d]	0.0151	0.503 ± 0.011	0.472 ± 0.009	0.368 ± 0.009	0.267 ± 0.008	0.127 ± 0.009	−1.64 ± 0.18	0.202 ± 0.024	23.6 ± 0.7	102.6 ± 18.2	0.6 ± 0.1
SNF20080720-001	0.0194	1.647 ± 0.227	1.184 ± 0.227	0.792 ± 0.227	0.538 ± 0.227	0.308 ± 0.227	0.61 ± 0.17	0.627 ± 0.016	12.8 ± 3.6	144.9 ± 3.8	0.6 ± 0.3
SNF20080802-006	0.0713	0.271 ± 0.036	0.297 ± 0.035	0.352 ± 0.035	0.303 ± 0.035	0.460 ± 0.036	−2.95 ± 0.53	−0.010 ± 0.031	23.8 ± 3.0	113.0 ± 6.7	−0.5 ± 0.1
SNF20080803-000	0.0571	0.303 ± 0.019	0.261 ± 0.016	0.183 ± 0.017	0.161 ± 0.016	0.173 ± 0.017	0.04 ± 0.16	0.143 ± 0.016	7.7 ± 2.1	117.9 ± 3.9	−1.1 ± 0.1
SNF20080810-001	0.0423	0.012 ± 0.031	0.089 ± 0.030	0.146 ± 0.030	0.081 ± 0.030	−0.003 ± 0.030	−1.52 ± 0.16	0.030 ± 0.019	23.8 ± 1.0	90.2 ± 22.9	−0.0 ± 0.1
SNF20080822-005	0.0705	−0.532 ± 0.052	−0.355 ± 0.052	−0.346 ± 0.052	−0.264 ± 0.051	−0.197 ± 0.052	0.35 ± 0.26	−0.005 ± 0.017	7.3 ± 1.4	79.9 ± 3.5	1.1 ± 0.5
SNF20080825-010	0.0396	−0.198 ± 0.057	−0.134 ± 0.057	−0.102 ± 0.057	−0.120 ± 0.056	−0.165 ± 0.057	−1.34 ± 0.23	0.037 ± 0.021	19.5 ± 1.8	102.8 ± 14.1	0.8 ± 0.2
SNF20080909-030	0.0298	−0.139 ± 0.033	−0.139 ± 0.032	−0.166 ± 0.032	−0.115 ± 0.032	−0.154 ± 0.033	0.87 ± 0.16	0.073 ± 0.020	8.2 ± 1.2	92.3 ± 2.1	0.8 ± 0.2
SNF20080913-031	0.0540	0.087 ± 0.042	−0.013 ± 0.041	−0.015 ± 0.041	0.011 ± 0.041	−0.053 ± 0.041	−0.19 ± 0.18	0.080 ± 0.020	10.0 ± 1.6	117.8 ± 2.4	0.0 ± 0.0
SNF20080914-001	0.0235	0.498 ± 0.020	0.348 ± 0.017	0.195 ± 0.017	0.139 ± 0.016	−0.007 ± 0.017	−1.12 ± 0.17	0.205 ± 0.024	16.1 ± 1.2	129.6 ± 3.1	1.0 ± 0.1
SNF20080918-000	0.0661	0.417 ± 0.038	0.323 ± 0.037	0.173 ± 0.037	0.176 ± 0.037	0.167 ± 0.037	1.19 ± 0.31	0.176 ± 0.021	7.4 ± 3.7	152.6 ± 5.5	−0.8 ± 0.4
SNF20080918-002	0.0857	−0.286 ± 0.048	−0.086 ± 0.047	−0.014 ± 0.047	0.021 ± 0.047	0.091 ± 0.057	−1.12 ± 0.15	−0.059 ± 0.014	16.4 ± 2.5	100.8 ± 4.5	0.1 ± 0.2
SNF20080918-004	0.0499	0.223 ± 0.221	0.177 ± 0.221	0.217 ± 0.221	0.222 ± 0.221	0.232 ± 0.221	−2.07 ± 0.30	−0.042 ± 0.026	24.3 ± 1.7	90.4 ± 8.3	−0.1 ± 0.3
SNF20080919-001	0.0409	−0.526 ± 0.028	−0.467 ± 0.027	−0.482 ± 0.028	−0.422 ± 0.027	−0.446 ± 0.028	0.44 ± 0.18	0.059 ± 0.017	5.1 ± 0.5	83.5 ± 1.2	−0.2 ± 0.1
SNF20080919-002	0.0547	0.486 ± 0.020	0.583 ± 0.017	0.591 ± 0.018	0.518 ± 0.017	0.440 ± 0.036	−2.77 ± 0.35	0.064 ± 0.034	31.4 ± 4.1	107.4 ± 22.3	−2.0 ± 0.2
SNF20080920-000	0.0390	−0.161 ± 0.078	−0.196 ± 0.077	−0.241 ± 0.077	−0.180 ± 0.077	−0.174 ± 0.077	0.82 ± 0.24	0.092 ± 0.020	5.6 ± 3.7	137.9 ± 3.3	−1.3 ± 0.3
PTF09dlc[i]	0.0663	−0.255 ± 0.036	−0.208 ± 0.035	−0.157 ± 0.035	−0.118 ± 0.035	−0.071 ± 0.035	−0.07 ± 0.11	−0.010 ± 0.010	12.9 ± 1.2	143.9 ± 3.0	−0.7 ± 0.2
PTF09dnp[i]	0.0376	−0.491 ± 0.060	−0.242 ± 0.059	−0.138 ± 0.059	−0.227 ± 0.059	−0.369 ± 0.059	−1.62 ± 0.29	−0.024 ± 0.023	16.8 ± 1.1	65.5 ± 8.3	−1.3 ± 0.3
PTF09fox[i]	0.0706	−0.248 ± 0.033	−0.185 ± 0.033	−0.074 ± 0.033	0.025 ± 0.033	0.210 ± 0.033	−0.21 ± 0.23	−0.104 ± 0.013	9.4 ± 1.4	123.8 ± 2.7	0.4 ± 0.2
PTF09foz[i]	0.0532	−0.007 ± 0.043	−0.080 ± 0.043	−0.063 ± 0.043	−0.121 ± 0.043	−0.127 ± 0.043	−1.53 ± 0.31	0.053 ± 0.023	22.7 ± 1.2	127.4 ± 2.6	0.8 ± 0.3

Notes. Discovery: [a]Boles, Armstrong; [b]LOSS ; [c]Sloan Digital Sky Survey II; [d]Prasad, Li (LOSS); [e]Orff, Newton; [f]Parisky, Li (LOSS); [g]Monard; [h]Quimby et al.; [i]PTF. Discovery attribution was obtained from http://www.cfa.harvard.edu/iau/lists/Supernovae.html and the CBAT. [1]Redshifts are taken from Cooke et al. (2011) and Childress et al. (in prep.).